This article was downloaded by: [Tomsk State University of Control Systems and Radio]
On: 20 February 2013, At: 13:23
Publisher: Taylor & Francis
Informa Ltd Registered in England and Wales Registered Number: 1072954 Registered office: Mortimer House, 37-41 Mortimer Street, London W1T 3JH, UK

Molecular Crystals and Liquid Crystals
Publication details, including instructions for authors and subscription information:
http://www.tandfonline.com/loi/gmcl16

A Molecular Dynamics Simulation of an ODIC Phase

M. Yvinec [a b]

[a] Département de Recherches Physiques,[†;] , Université Pierre et Marie Curie, 4 Place Jussieu, 75230, PARIS, CEDEX 05 France

[b] L.A.n°71 (C.N.R.S.)

Version of record first published: 20 Apr 2011.

To cite this article: M. Yvinec (1984): A Molecular Dynamics Simulation of an ODIC Phase, Molecular Crystals and Liquid Crystals, 109:2-4, 303-340

To link to this article: http://dx.doi.org/10.1080/00268948408078715

PLEASE SCROLL DOWN FOR ARTICLE

Full terms and conditions of use: http://www.tandfonline.com/page/terms-and-conditions

This article may be used for research, teaching, and private study purposes. Any substantial or systematic reproduction, redistribution, reselling, loan, sub-licensing, systematic supply, or distribution in any form to anyone is expressly forbidden.

The publisher does not give any warranty express or implied or make any representation that the contents will be complete or accurate or up to date. The accuracy of any instructions, formulae, and drug doses should be independently verified with primary sources. The publisher shall not be liable for any loss, actions, claims, proceedings, demand, or costs or damages whatsoever or howsoever caused arising directly or indirectly in connection with or arising out of the use of this material.

Mol. Cryst. Liq. Cryst., 1984, Vol. 109, pp. 303–340
0026-8941/84/1094–0303/$18.50/0
© 1984 Gordon and Breach, Science Publishers, Inc.
Printed in the United States of America

Downloaded by [Tomsk State University of Control Systems and Radio] at 13:23 20 February 2013

A Molecular Dynamics Simulation of an ODIC Phase

M. YVINEC

Département de Recherches Physiques,† Université Pierre et Marie Curie, 4 Place Jussieu, 75230 PARIS CEDEX 05 (France)

(*Received November 23, 1983; in final form March 12, 1984*)

This paper is the second of a series devoted to a molecular dynamics study of a two dimensional ODIC crystal which can be viewed as the schematization of the real 3d plastic NaCN. In this paper we are mainly concerned with some static and dynamical properties of the model namely the translational lattice phonons, the correlations between neighbouring molecules orientations, the collective behaviour of the reorientational processes and the influence of the rotation-translation coupling effect. This last effect being strongly dependent on the characteristic times of the rotational dynamics compared to the inverse frequencies of the translational lattice modes, we have run two different molecular dynamics experiments with two different values of the moment of inertia of the dumbbells which in our model figure the CN^- ions. The relevant collective correlation functions have then been computed and the outcoming informations are analysed and compared with the results of the presently available theories of Y. Yamada and of K. H. Michel which both assume a linear orientation-translation coupling.

I. INTRODUCTION

The rotation-translation coupling is known to be an important feature for a large class of molecular crystals. This coupling is mostly important in the high temperature disordered phases, named ODIC, where the centers of mass still form a regular lattice while molecular orientations already display some disorder. Indeed, in those phases, the rotational dynamics involve both librational oscillations around some preferred orientations and large amplitude reorientations from one preferred orientation to another. However, the steric hindrance in the crystal generally implies that a reorientational process should

†L.A.n°71 (C.N.R.S.).

occur simultaneously with a displacement of the centers of mass of neighbouring molecules. The high temperature cubic phases of alkali cyanides (NaCN, KCN, RbCN and CsCN) are well known examples of such ODIC phases with strong rotation-translation coupling. Experimental evidence of this coupling arises from ultrasonic,[1] Brillouin[2] and neutron[3] scattering data which show an anomalous upward curvature of the transverse acoustic branch in the [100] direction of the wavevector and a critical softening of the shear elastic constant C_{44} as the transition temperature to a more ordered phase is approached.

From a theoretical point of view, the description of ODIC phases is complicated by the lack of well defined equilibrium positions and the large amplitude rotations of the molecules. In their work on the structural phase transitions in molecular crystals, Y. Yamada *et al.*[4] described the rotational dynamics through a pseudo-spin stochastic variable. More recently, K. H. Michel *et al.*[5-7] used symmetry adapted functions of the angular coordinates to describe both the static and dynamical properties of such systems. In both cases, the translation-rotation coupling was described through a bilinear term involving the orientational variables and the normal coordinates of the phonon lattice modes.

In other respects, the recent improvement of computer efficiency allows to perform numerical simulations which appear to be precious tools in the study of disorder system in general and ODIC phases in particular. For example, M. L. Klein and J. J. Weis[8,9] performed a molecular dynamics simulation of the disordered (or β) solid phase of N_2. G. S. Pawley and G. W. Thomas[10] used the full power of a distributed array processor to simulate a large crystal of SF_6 allowing to study the plastic to crystalline phase transition. M. L. Klein *et al.* have performed a series of numerical simulations of the high temperature alkali cyanide crystals RbCN,[11] CsCN,[12] NaCN and KCN.[13,14] These authors used a simple model of interionic forces which includes an atom–atom (exp. 6) potential plus coulomb forces and succeeded in reproducing the main features of alkali cyanides, particularly the anomalous softening of the transverse acoustic branches in the [100] wavevector direction. Furthermore, they made clear that the charge distribution of the CN^- ions has a crucial influence on the shape of the static orientational probability density function. In one paper of this series, R. M. Lynden-Bell and M. L. Klein[14] performed a theoretical analysis of the translation-rotation coupling as it appears in their system and showed that a Mori type approach similar to the theory developed by K. H. Michel provided a good description of the dynamics of the simulated crystal.

Downloaded by [Tomsk State University of Control Systems and Radio] at 13:23 20 February 2013

Downloaded by [Tomsk State University of Control Systems and Radio] at 13:23 20 February 2013

The preceding approach has as an objective to reproduce as closely as possible, all the known experimental facts on the alkali cyanides. The 3d aspect of the calculation, as well as the best quality of the potential were thus two prerequisites of these calculations. The price which had then to be paid was the small size of the specimen understudy, and thus the very small number of independent points in the Brillouin zone which could be reached. In this as well as in the first paper of this series[15] (hereafter referred to as I) we have decided to take a different philosophy. Having in mind to study specifically the reorientational processes and the related translation-rotation coupling, we have chosen to perform molecular dynamics simulations for a simple 2d model which can be regarded as a 2d schematization of plastic NaCN. The choice of a 2d model made the computational work faster which allowed us to simulating a relatively large sample of 10×10 unit cells (instead of the $2 \times 2 \times 2$ or $3 \times 3 \times 3$ fcc sample in Klein *et al.* calculation) providing thus information about points of the Brillouin zone with a spacing of one tenth of the reciprocal lattice. Furthermore, it is clear (*see e.g.*[4,6,7]) that the important physical quantity which governs the translation-rotation coupling is $\omega_{\vec{q}}\tau_0$, where $\omega_{\vec{q}}$ is the frequency of the involved translational phonon, and τ_0 a characteristic time of the individual reorientation process. To study the related effects, we have chosen to vary arbitrarily, I, the moment of inertia of the dumbbell (which corresponds to the CN^- ion in our calculation), leaving all other quantities unchanged. Two different computations have thus been performed, one with a value of I typical of the actual NaCN situation i.e. $\omega_{\vec{q}}\tau_0 \simeq 1$ for zone boundary acoustical phonons, the other one for a value of I 8 times larger, so that only zone center acoustical phonons match the $\omega_{\vec{q}}\tau_0 \simeq 1$ condition. The purpose of the present paper which is just the following of I is to describe the results obtained in our numerical study of these models, for both some typical static and dynamical correlation functions.

Before coming to these results (in parts IV–VI), we shall first, in part II, recall the main features of the simulated model and give a short presentation of the two numerical experiments. Then, in part III, we recall briefly the main results of the Glauber Yamada[4] theory concerning the linear pseudospin-phonon coupled systems, results which can serve as a guideline in the description and interpretation of the numerical data arising from our simulations. In part IV the dispersion curves and the linewidths of the phonon lattice modes are discussed. Part V is devoted to the study of the static orientational correlations which appear to be strongly anisotropic and directed along the [01] and [10] crystal axis. The collective behaviour of the

reorientational processes appear in the wave number and frequency dependence of the rotational correlation functions which are presented in part VI, and compared with the central component arising in the spectrum of certain translation-translation correlation functions due to the coupling between reorientations and translations. Finally, in the appendix, the theoretical treatment of K. H. Michel *et al.* is applied to our system and in particular we give an estimation of the linear translation-rotation coupling coefficient.

II. THE MODEL AND THE TWO MOLECULAR DYNAMICS EXPERIMENTS

a) The simulated system can be described as a two dimensional ionic compound A^+XY^-, where the anion XY^- is a rigid, symmetric, dumbbell of length d which is bound to lie in the plane of the system. Our model includes only pair interactions which are coulomb forces and short range repulsive forces. The short range repulsive forces are limited to the interaction between each end of the XY^- ions and the

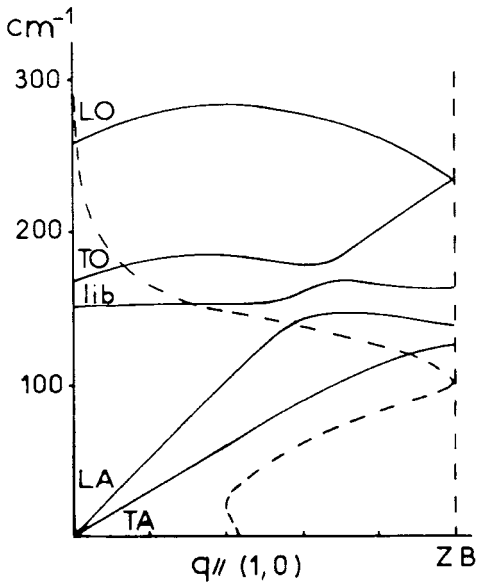

FIGURE 1a Characteristic frequencies in the case of the light moment of inertia (case of RUN A); full line: dispersion curves for the low temperature ferroelastic structure ($\bar{q}//[10]$); dashed line: density of librational excitations in the case of RUN A (arbitrary horizontal scale).

Downloaded by [Tomsk State University of Control Systems and Radio] at 13:23 20 February 2013

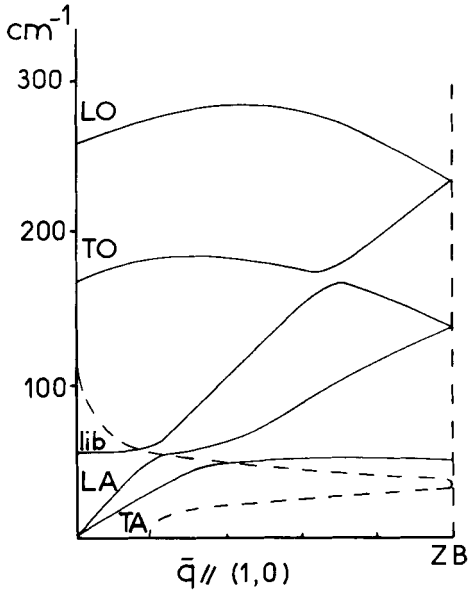

FIGURE 1b Characteristic frequencies in the case of the heavy moment of inertia (case of RUN B); full line: dispersion curves for the low temperature ferroelastic structure ($\bar{q}//[10]$); dashed line: density of librational excitations in the case of RUN B (arbitrary horizontal scale).

surrounding A^+ ions. The dumbbell XY^- is assumed to have a head and tail symmetry and this interaction derives from a Born Mayer atom–atom potential of the form $\lambda e^{-r/r_0}$. As far as coulomb forces are concerned, each ion, A^+ or XY^-, is considered as a monopole of charge $\pm q$ located at the center of mass, as the higher moments of the charge distribution are neglected the electrostatic part of the potential is independent of the molecular orientations; it is to be noted that, with such a system of interactions, there is no direct coupling between the orientations of neighbouring dumbbells.

The exact low temperature structure corresponding to that model is not known and may in fact be rather complicated, and includes many formular units in the unit cell. However, we have shown in I, that starting from a simple Bravais square lattice which is unstable a ferroelastic shear distortion leads to a structure dynamically stable at least in the harmonic approximation. In this structure the basis vectors of the Bravais lattice have an equal length ($a \simeq 3.88$ Å) and form an angle of 82°, the XY^- dumbbells being aligned along the longest diagonal of the unit cell. In fact, this ferroelastic distorted structure is

Downloaded by [Tomsk State University of Control Systems and Radio] at 13:23 20 February 2013

certainly a realistic approximation for the actual structure of the low temperature phase of the simulated crystal.

b) The simulation uses the classical molecular dynamics technique. The simulated crystal includes an original sample of 10 × 10 unit cells (100 formular unit $A^+ XY^-$) which is periodically repeated in the usual way. The coulomb interaction is handled via the method of

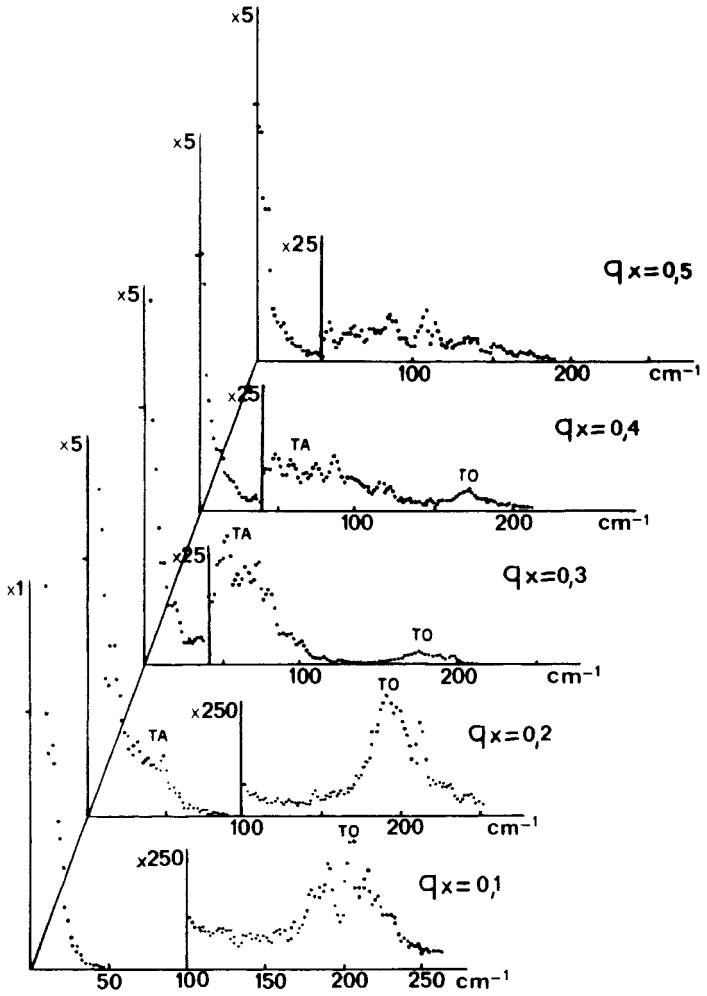

FIGURE 2a The power spectra $U_+(\bar{q}, \omega)$ relative to the transverse displacement of the A^+ ions. The wave vector $\bar{q}$ is parallel to the direction [10] and its component q_x is indicated in unit of $2\pi/a$. The indicated vertical scales correspond to an arbitrary unit. *Figure 2a* is relative to the RUN A experiment.

Downloaded by [Tomsk State University of Control Systems and Radio] at 13:23 20 February 2013

Ewald sums[16] and the equations of motion are integrated through the standard Verlet algorithm[17] with a time step of 10^{-14} s. This time step is approximately one tenth of the shortest characteristic evolution time of the system (the highest optical frequency being slightly under 300 cm^{-1} as will be seen on the dispersion curves (*Figures 1a and 1b*)).

As already mentioned in the introduction, the results presented below concern two different molecular dynamics experiments. In the first one, called RUN A, the moment of inertia of the XY^- dumbbells

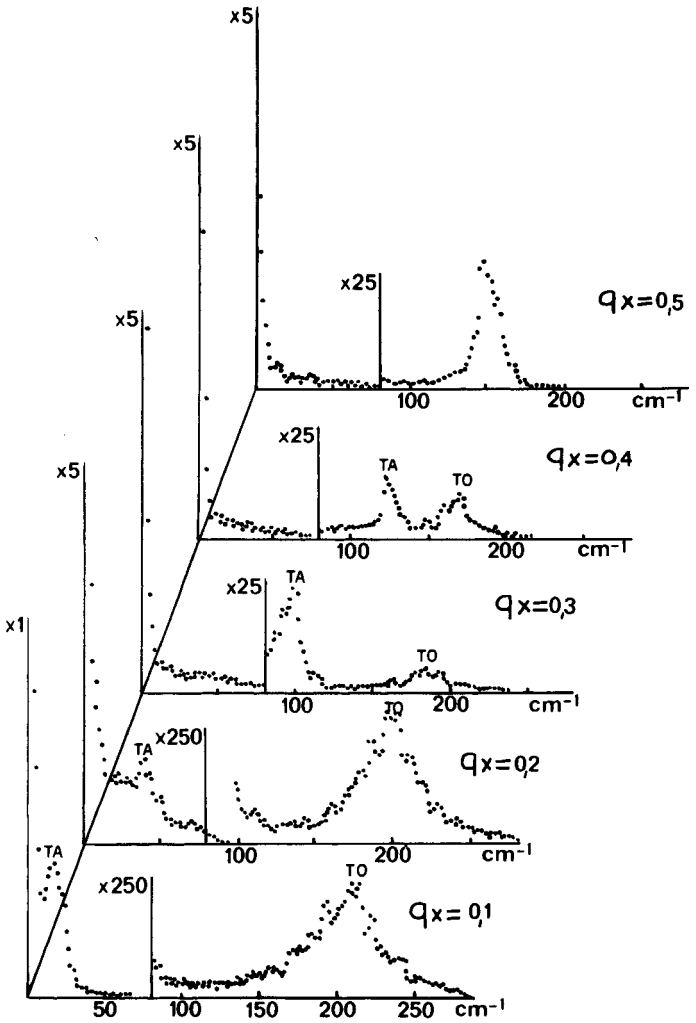

FIGURE 2b Same as Figure 2a relative to the RUN B experiment.

Downloaded by [Tomsk State University of Control Systems and Radio] at 13:23 20 February 2013

was assigned a numerical value such that the mean librational frequency (about 120 cm^{-1}) would match with the frequency range of the zone boundary phonons. In the second one, RUN B, this moment of inertia was modified by a factor 8 so that the librational frequencies match only with the acoustical phonon branches near the zone center (*cf. Figure 1*). Furthermore, RUN A corresponds to a kinetic temperature of about 300 K and RUN B to a temperature of 400 K, temperatures at which the system was actually found to be in a disordered ODIC phase. RUN A was carried out on a Cyber 750 computer and included in fact two independent experiments, each of which, after a few hundred steps of thermalization, was run over 5120 steps. RUN B includes 20 000 steps after thermalization and was carried out on the Cray 1 computer of the CCVR. The numerical value used for the potential parameters and the thermodynamic characteristics of the two runs are listed in Tables I and II.

Table II also contains the root mean square displacements of the centers of mass ($\sqrt{\langle u_+^2 \rangle}$ and $\sqrt{\langle u_-^2 \rangle}$) obtained in our simulation for both ion species. These values can be compared with the corresponding Debye Waller factor computed for the ferrodistorted (low temperature) ordered structure, at the same temperatures (300 K and 400 K), through an harmonic approximation. The values obtained in the molecular dynamics simulations are approximately twice as large as those deduced from the ordered ferrodistorted phase, though, as we shall see in part IV, the translational phonon frequencies have approximately the same values. This fact already stresses the importance of the translation-rotation coupling, the additional contribution to the

TABLE I

Numerical values of the different parameters used as input data in the computer simulation

Coulomb interaction	$q = 1.6\ 10^{-19}$C
	$\frac{q^2}{4\pi\epsilon_0} = 14.42$ eVÅ
repulsive interaction $\lambda e^{-r/r_0}$	$\lambda = 459.5$ eV
	$r_0 = 0.328$ Å
length of the dumbbell XY^-	$d = 0.6$ Å
Kinetic parameters	
masses	$m_+ = m_- = 25$ u.ma
inertial moment	RUN A $I = 2 \times m_- \frac{d^2}{4}$
of the dumbbell	RUN B $I = 16 \times m_- \frac{d^2}{4}$

Downloaded by [Tomsk State University of Control Systems and Radio] at 13:23 20 February 2013

TABLE II

Some thermodynamic characteristics of the two molecular dynamics runs[a]

	T/K	U/N(eV)	PS/NkT	$\sqrt{\langle u_+^2\rangle}$(Å)	$\sqrt{\langle u_-^2\rangle}$(Å)
RUN A	310	−7.442	3.68	0.39 (0.160)	0.35 (0.160)
RUN B	390	−7.425	4.49	0.36 (0.162)	0.33 (0.162)

[a]Temperature T, mean potential energy per formular unit U/N, the two dimensional pressure factor PS/NkT and the mean square displacements $\sqrt{\langle u_+^2\rangle}$ and $\sqrt{\langle u_-^2\rangle}$. The values given in parenthesis for the mean square displacement corresponds to the values obtained at the same temperature for the ordered ferroelastic structure in the harmonic approximation.

Debye Waller factor in the plastic phase being due to the large low frequency displacements of the centers of mass involved in the reorientation processes owing to the steric hindrance in the crystal.

c) the dynamical behaviour of the simulated crystal was investigated through a set of collective wave vector dependent variables which were chosen to be

either ■ translational variables

$$\bar{u}_{\pm}(q,t) = \frac{1}{\sqrt{N}}\sum_L e^{i\bar{q}\cdot\bar{X}_{L\pm}}\bar{u}_{\pm}(L,t) \qquad \text{(II-1)}$$

or ■ rotational variables

$$f(q,t) = \frac{1}{\sqrt{N}}\sum_L e^{i\bar{q}\cdot\bar{X}_L} f(\theta_L,t) \qquad \text{(II-2)}$$

L labels the N different unit cells in the original sample, + or − indexes the two ions in the unit cell,

$\bar{u}_{\pm}(L,t)$ is the displacement of the center of mass of the $L_{\pm}$ ions, from its mean position $\bar{X}_{L_{\pm}}$,

and θ_L is the angular coordinate of the dumbbell XY^- of the L cell.

Let us simply recall here that we have shown in I that the mean position $\bar{X}_{L_{\pm}}$ form a square lattice, and that the dumbbell XY^- have two preferred orientations which in the crystal square axes are the directions [11] (i.e. $\theta = \pi/4$ modulo π) and [1$\bar{1}$] (i.e. $\theta = 3\pi/4$ modulo π). We have also shown in I, that the most interesting orientational functions $f(\theta_L)$ fall into two categories: those which, as

Downloaded by [Tomsk State University of Control Systems and Radio] at 13:23 20 February 2013

$\cos 2\theta_L$, essentially show the librational motion of the dumbbells around their preferred orientations and those which are essentially sensitive to the reorientational motions, like $\sin 2\theta_L$ or, even better, the associated pseudo spin:

$$\sigma_2(L) \equiv \sigma_2(\theta_L) = 1 \times \text{sign of } \sin(2\theta_L) \tag{II-3}$$

Now the size of the original sample being 10×10 unit cells, the different wavevectors available from the molecular dynamics data form a sublattice of the reciprocal space, the spacing of which is one tenth of the reciprocal Bravais lattice. The treatment of molecular dynamics data then essentially consist in computing the average correlations.

$$\langle \bar{u}_{\pm}(\bar{q}, t+\tau)\bar{u}^*_{\pm}(\bar{q}, t)\rangle \tag{II-4}$$

$$\langle f(\bar{q}, t+\tau), f^*(\bar{q}, t)\rangle \tag{II-5}$$

and their Fourier transform (via an FFT procedure) to get the translation and orientational power spectra

$$\bar{\bar{U}}_{\pm}(\bar{q}, \omega) = \int e^{-i\omega\tau} d\tau \langle \bar{u}_{\pm}(\bar{q}, t+\tau)\bar{u}^*_{\pm}(\bar{q}, t)\rangle \tag{II-6}$$

$$F(\bar{q}, \omega) = \int e^{-i\omega\tau} d\tau < f(\bar{q}, t+\tau) f^*(\bar{q}, t)\rangle \tag{II-7}$$

III. THEORETICAL TREATMENTS, A VERY BRIEF REVIEW

As mentioned in the introduction, from a theoretical point of view, the description of the dynamics of plastic crystals is extremely difficult. Indeed,

- small (librations) and large (reorientations) angular rotations have to be considered at the same time,
- reorientation-translation coupling involves important changes in the positions of the centers of mass so that small and large amplitude motions of the latter have also to be considered simultaneously.

The analysis of the dynamical data usually relies on the over-simplified pseudospin–phonon linear coupling theory of Glauber–Kubo, Yamada *et al.*[4]. Because of its great simplicity and of its ability to serve as a guideline for the description of our results we recall here some of the main features of this theory.

Downloaded by [Tomsk State University of Control Systems and Radio] at 13:23 20 February 2013

Downloaded by [Tomsk State University of Control Systems and Radio] at 13:23 20 February 2013

Following Yamada *et al.*[4] the free energy of the coupled pseudospin-phonon system is written under the form

$$F = F_0 + \sum_{j\bar{q}} \left(\frac{1}{2}\omega_j^2(\bar{q}) u_j(\bar{q}) u_j^*(\bar{q}) + \frac{1}{2} g(\bar{q}) \sigma(\bar{q}) \sigma^*(\bar{q}) + d_j(\bar{q}) u_j(\bar{q}) \sigma^*(\bar{q}) \right) \tag{III-1}$$

where

$u_j(\bar{q})$ is the normal coordinate of a phonon (indexed with the wave-vector $\bar{q}$ and a branch index j)

$\sigma(\bar{q})$ is a collective pseudospin variable, spatial Fourier transform of II-3.

The first term in (III-1) is the usual free energy of a phonon system, the second term representing the free energy of the pseudospin system. Following Glauber and Kubo master equation technique, $g(\bar{q})$ may be written as $kT - J(\bar{q})$ where $J(\bar{q})$ represents in their original work a bilinear coupling between the pseudospin. In fact, for a limited range of temperature, even when this coupling has a more complex form, $J(\bar{q})$ can be viewed as a renormalized effective, temperature dependent, coupling coefficient. The last term of III-1 represents an assumed *bilinear* coupling between the pseudospin and the phonon variables. The numerical relative importance of this linear coupling term strongly depends on the problem under study and will be shortly discussed at the end of this section.

If one assumes, for the pseudospin, a diffusive dynamics with a relaxation time τ_0, the Green functions for the coupled system are found from the inverse of the following dynamical matrix

$$G^{-1}(\omega) = \begin{bmatrix} \omega_{\bar{q}}^2 - \omega^2 & d(\bar{q}) \\ d^*(\bar{q}) & g(\bar{q}) - i\gamma_0\omega \end{bmatrix} \tag{III-2a}$$

with

$$\gamma_0 = kT\tau_0 \tag{III-2b}$$

Here and in the following, we have dropped the j index of the coupled phonon branch and written simply $\omega_{\bar{q}}$ for the bare phonon frequency $\omega_j(\bar{q})$. Thus, the Fourier spectra $\Sigma(\bar{q}, \omega)$ and $U(\bar{q}, \omega)$ of respectively the spin–spin correlation functions and the phonon-pho-

non correlation functions are given by:

$$\Sigma(\bar{q},\omega) = \frac{kT}{\omega}\mathrm{Im}G_{\sigma\sigma}(\bar{q},\omega) \tag{III-3a}$$

$$= \frac{\tau_0}{\left[\frac{1}{kT}\left(g(\bar{q}) - \frac{d(\bar{q})d^*(\bar{q})}{\omega_{\bar{q}}^2 - \omega^2}\right)\right]^2 + \omega^2\tau_0^2} \tag{III-3b}$$

and

$$U(\bar{q},\omega) = \frac{kT}{\omega}\mathrm{Im}G_{uu}(\omega) \tag{III-4a}$$

$$= \frac{kT}{\omega}\mathrm{Im}\left(\frac{1}{\omega_{\bar{q}}^2 - \frac{d(\bar{q})d(\bar{q})^*}{g(\bar{q})}\left(\frac{1}{1 - i\frac{\gamma_0\omega}{g(\bar{q})}}\right) - \omega^2}\right) \tag{III-4b}$$

$$= \frac{d(\bar{q})d^*(\bar{q})}{\left(\omega_{\bar{q}}^2 - \omega^2\right)^2}\Sigma(\bar{q},\omega) \tag{III-4c}$$

These formulae are essentially useful in two extreme regimes: the case of fast relaxation of the spin system ($\omega_{\bar{q}}\tau_0 \ll 1$) and the case of slow relaxation ($\omega_{\bar{q}}\tau_0 \gg 1$).

In the case of fast relaxation ($\omega_{\bar{q}}\tau_0 \ll 1$), the spin system follows adiabatically the phonon response. The damping term $\gamma_0\omega/g(\bar{q})$ in IIII-4b is unimportant and there is a critical softening of the frequency of the slow phonon strongly coupled to the reorientation motion.

In the case of slow relaxation ($\omega_{\bar{q}}\tau_0 \gg 1$) the phonon system propagates into an essentially fixed disordered crystal. The phonon response functions $U(\bar{q},\omega)$ exhibits the characteristic three peaks structure with a quasi unshifted phonon side peak in addition to a central resonance which appears also in the pseudospin response function $\Sigma(\bar{q},\omega)$. Formulae (III-3b) and (III-4c) show that in that case $\Sigma(\bar{q},\omega)$ and the central component of $U(\bar{q},\omega)$ have parallel lorentzian lineshapes:

$$\omega \ll \omega_{\bar{q}}\ \Sigma(\bar{q},\omega) = \frac{1}{\frac{1}{kT}\left(g(\bar{q}) - \frac{d(\bar{q})d^*(\bar{q})}{\omega_{\bar{q}}^2}\right)}\frac{\tau(\bar{q})}{1 + \omega^2\tau^2(\bar{q})} \tag{III-5}$$

Downloaded by [Tomsk State University of Control Systems and Radio] at 13:23 20 February 2013

and

$$\omega \ll \omega_{\bar{q}}\, U(\bar{q},\omega) = \frac{1}{\omega_{\bar{q}}^2}\frac{d(\bar{q})d^*(\bar{q})}{\omega_{\bar{q}}^2}\Sigma(\bar{q},\omega) \qquad \text{(III-6)}$$

with an effective correlation time

$$\tau(\bar{q}) = \frac{\tau_0}{\dfrac{1}{kT}\left(g(\bar{q}) - \dfrac{d(\bar{q})d^*(\bar{q})}{\omega_{\bar{q}}^2}\right)} \qquad \text{(III-7)}$$

We shall see in the following sections that, roughly, our simulated system realizes either the case of slow relaxation ($\omega_{\bar{q}}\tau_0 \gg 1$) or the more complex intermediate case which corresponds to the conditions $\omega_{\bar{q}}\tau_0 \simeq 1$. In fact, the limited size of the simulated sample does not allow to reach cases of fast relaxation which should obviously occur for very small wavevectors.

Let us finally discuss briefly the microscopic origin of the three types of terms which appear in III-1.

■ The first term is a direct, spin independent, displacement–displacement interaction, and we shall see in IV-b how this quantity can be actually computed in our model.

■ The value of the coefficient $d(\bar{q})$ can be obtained by using the more sophisticated theory of Michel and Naudts.[5,6] In view of its relative complexity the calculation is done in the Appendix, where it is shown that the function $\sin 2\theta$ (which does not much differ from the pseudospin II-3) couples merely to the acoustic phonons, this coupling having the form

$$B_2\left(\cos\frac{q_x a}{2}\sin\frac{q_y a}{2}u^x(q) + \sin\frac{q_x a}{2}\cos\frac{q_y a}{2}u^y(q)\right)\sin 2\theta \qquad \text{(III-8)}$$

■ The microscopic origin of the direct $\bar{q}$ dependent spin–spin interaction which appears in (III-1) presents a more important difficulty. Indeed, the type of interactions (Born Mayer interaction between the ends of the dumbbells and the A^+ ion) used in our model does not lead to a direct interaction between neighbouring spins. Furthermore, the Michel and Naudts formalism leads, in the original form (*see* A-4 and A-26) to a purely local ($\bar{q}$ independent) interaction between the spins. Nevertheless, as we shall see in parts V and VI, the use of the theoretical results of this section in the interpretation of our

Downloaded by [Tomsk State University of Control Systems and Radio] at 13:23 20 February 2013

numerical results implies a $\bar{q}$ dependence and a strong anisotropy of $J(\bar{q})$. This means that the effective $J(\bar{q})$ that we shall use in the discussion of our simulation cannot be derived, from our microscopic model, by the simple theories presently available.

IV. THE PHONON LATTICE MODES

a) The computed displacement – displacement correlation functions

The transverse and longitudinal displacement–displacement correlation functions $U^{t}_{\pm}(\bar{q}, \omega)$ have been computed for $\bar{q}$ wavevectors along the [10] and [11] directions. For example, Figure 2 shows the correlation functions relative to the transverse motion of the A^+ ions with wavevectors parallel to the [10] direction. The phonon lattice modes appear generally as relatively well defined underdamped resonances of the response functions $U(\bar{q}, \omega)$ though some of them have a rather important linewidth. The main exception to this rule is the lowest transverse acoustic mode in the [10] wavevector direction ($\bar{q}$ = [0.1.0] in unit of $2\pi/a$) which, in the case of RUN A, is lost in the wing of a central resonance. In fact an important central resonance appears in addition to the phonon peak in all the transverse spectra relative to the [10] wavevector direction. A far less important central peak appears also in the longitudinal [11] spectra when the wavevector is nearly halfway to zone boundary. This central resonance reflects the importance of the coupling between the reorientational motion and the [10] TA phonons. The phonon reorientation coupling is indeed responsible for the anomalous behavior of the [10] TA phonon branch that we shall describe in IV c. First, we shall comment in IV b about the dispersion curves and phonon linewidths for the other branches which are not (or only weakly) coupled to the rotational motions.

b) Behaviour of the "normal" phonon branches

The dispersion curves and linewidths of the lattice modes are shown in Figure 3a (RUN A) and 3b (RUN B). It appears that, except for the low frequency [10] TA branch, these dispersion curves are well defined and very reminiscent of that of the low temperature phase. This result can be easily explained as follows. In our model, the force constants relative to the centers of mass motion are largely dominated by the long range Coulomb interactions which do not depend much on the local arrangement of the ions. The influence of the disorder appears mostly through the short range repulsive Born Mayer potential which

Downloaded by [Tomsk State University of Control Systems and Radio] at 13:23 20 February 2013

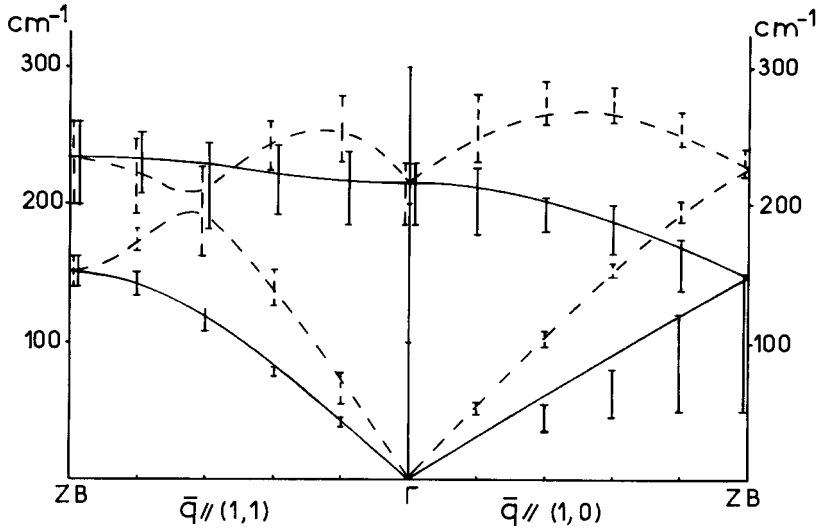

FIGURE 3a The translational phonon dispersion curves in the case of RUN A. The vertical bars represent the FWHM of the phonons peaks in the molecular dynamics experiment while the drawn dispersion curves represent the mean field results for the phonon frequencies. The full lines drawings are related to the transverse phonons while the dashed line drawings concern the longitudinal ones.

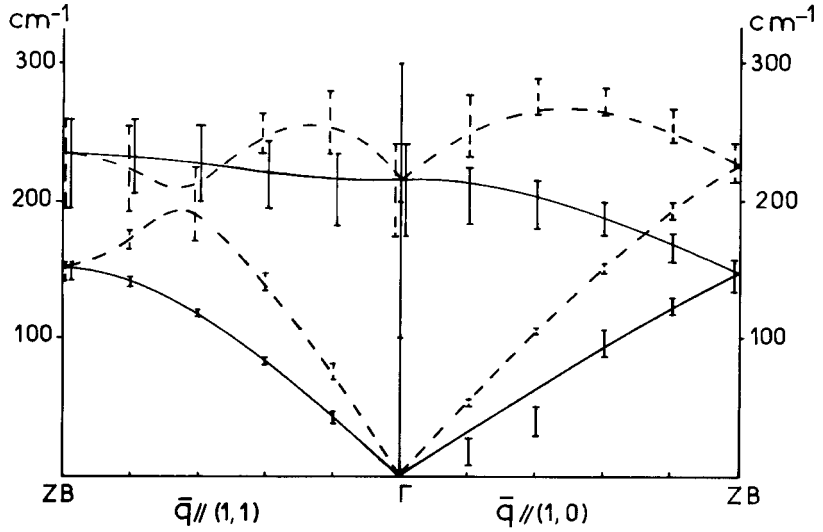

FIGURE 3b The translation phonon dispersion curves in the case of RUN B with the same conventions as in Figure 3a.

Downloaded by [Tomsk State University of Control Systems and Radio] at 13:23 20 February 2013

in our calculation acts only between nearest neighbour ions. Thus the effect of disorder on the phonon frequencies can be viewed as a perturbation with respect to the dispersion arising from the long range Coulomb interactions. With respect to that point of view, a zero order approximation for the phonon frequencies can be estimated in the following way: the equilibrium position of the centers of mass are assumed to be the mean square lattice positions and average harmonic force constants relative to the translational displacements are then derived from an averaging over the orientations of the XY^- dumbbells.†‡ This calculation leads to the dispersion curves which have been drawn as continuous lines in Figures 3a and 3b. For each value of the wavevector $\bar{q}$, and each "normal" phonon branch, the related phonon frequency fits well with the maximum of $U(\bar{q}, \omega)$ and can be viewed as an estimation for the bare phonon frequency $\omega_j(\bar{q})$ introduced in (III-1).

The linewidth of the phonon modes in the simulated plastic crystals has two distinct origins. The first one is related to the static aspect of the structural disorder (the plastic crystal being thus viewed as a molecular glass which is equivalent to postulating a slow relaxation regime), the other one being the lifetime of the structural fluctuations. Without relying on sophisticated methods, a direct measure of the first effect can be obtained by comparing for a given value of the wavelength ($|\bar{q}|$), the phonon frequencies obtained in the ferro distorted low temperature structure for two perpendicular directions of the wavevector. This should give an upper limit for the influence of the disorder, all the spins being in the ordered structure aligned in the same orientations. This procedure has been applied e.g. for $\bar{q}$ wavevectors parallel to the directions [11] and [1$\bar{1}$] (*see* Figure 4). For each wavelength and each polarization, the difference $(\omega_{11}(q) - \omega_{1\bar{1}}(q))$ is roughly proportional to the phonon linewidth (FWHM) obtained in the molecular dynamics simulation, even when this difference is large (typically, the ratio $2(\omega_{11}(q) - \omega_{1\bar{1}}(q))/(\omega_{11}(q) + \omega_{1\bar{1}}(q))$ may be of the order of 25%). With such an influence of the static aspect of the disorder on the phonon linewidth, the lifetime effect does not play an important role. The mean residence time of a molecule in its orienta-

†In our model, each ion is considered as an electrostatic monopole so that the averaging over molecular orientations concern only the short range (nearest neighbour) repulsive Born Mayer potential.

‡The averaging over molecular orientations should in principle involve the probability density function $P(\theta)$ derived in I from the molecular dynamics data. To make things easier we, here, have only taken into account the two most probable orientations [11] and [1$\bar{1}$], a simplification which should not change the result much.

Downloaded by [Tomsk State University of Control Systems and Radio] at 13:23 20 February 2013

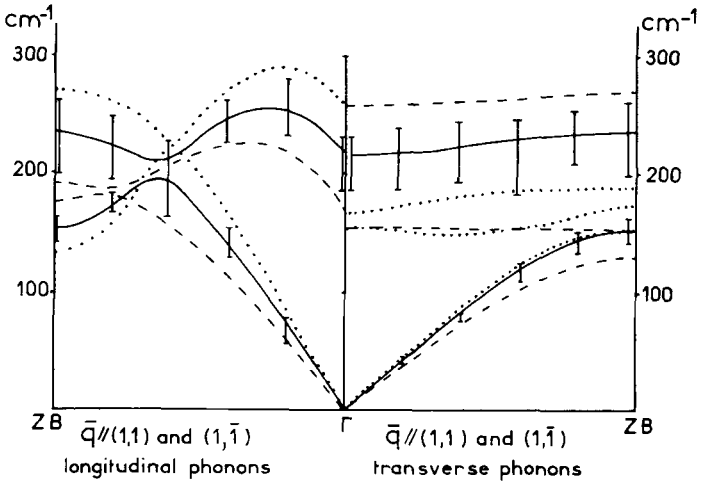

FIGURE 4 full line:—vertical bars: FWHM of the phonon peak in the molecular dynamics experiment (RUN A) for $\bar{q}//[11]$—mean field dispersion curves for $\bar{q}//[11]$; dotted line: dispersion curves of the ferroelastic ordered structure for $\bar{q}$ wavevectors along the [11] direction. dashed line: dispersion curves of the ferroelastic ordered structure for $\bar{q}$ wavevectors along the [11] direction.

tional potential well is approximately 1.3 pcs for RUN A (*see I*) and turns out to be 2.3 pcs for RUN B. This yields an additional contribution to the phonon linewidths of a few cm^{-1}, contribution which is negligible compared to linewidths arising from disorder effect.

c) Behaviour of the [10] TA branch

The theory of Yamada *et al.*, briefly reviewed in part III, implies that the phonon branches couple strongly to the reorientational processes whenever the coupling coefficient $d_j(\bar{q})$ is "important". A look at the Figure 5a helps in understanding why this is precisely the case for the [10] TA branch: the transverse phonons propagating in the [10] wavevector directions induce a shear distortion of the centers of mass lattices which obviously favors the reorientation of the dumbbells lying at the node of displacements. This geometrical argument is in agreement with the analysis of K. H. Michel which provides for the [10] TA phonons a coupling coefficient (*given in* III-8) which is maximum for zone boundary phonons. The coupling coefficient vanishes as $|q|$ goes to zero however this does not imply that the effect of the coupling vanishes as $|q|$ goes to zero. In fact, formula III-8 shows that, for each given wavevector direction in the small wave-

Downloaded by [Tomsk State University of Control Systems and Radio] at 13:23 20 February 2013

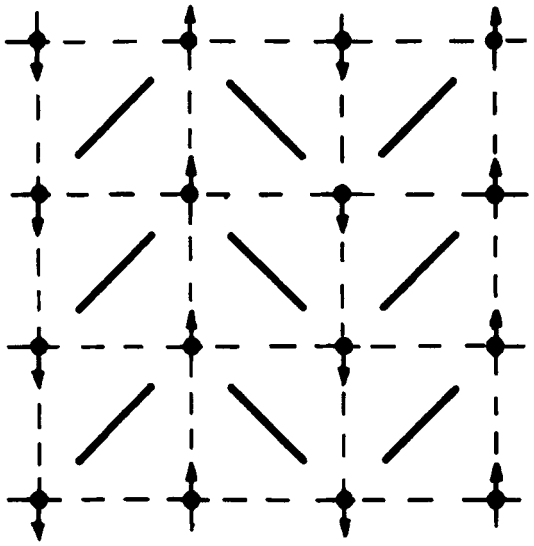

FIGURE 5a The displacement scheme of the A^+ ions for a transverse phonons propagating along the [10] direction.

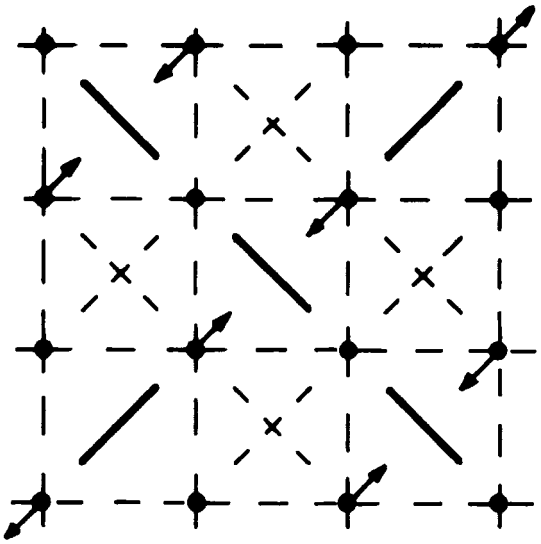

FIGURE 5b The displacement scheme of the A^+ ions for a longitudinal phonons propagating along the [11] direction.
In both The A^+ ions are represented in their mean position forming a square lattice and the arrows figure their displacements. The XY^- dumbbells are represented by a heavy bar in the preferred orientation which is favoured by the displacement, the two preferred orientations are drawn with dash lines when no one is favoured.

Downloaded by [Tomsk State University of Control Systems and Radio] at 13:23 20 February 2013

length limit, $d_j(\bar{q})$ is proportional to $|\bar{q}|$ so that the characteristic ratio $d_j(\bar{q})d_j^*(\bar{q})/\omega_j^2(\bar{q})$, appearing in formulae III-5, III-6 and III-7, behaves smoothly in the zone center region.†

Leaving for the part V, the discussion of the central resonance which appears in the response function $U(\bar{q}, \omega)$, we focus here on the phonon peak. The linear coupling theory of Yamada provided in the case of slow relaxation ($\omega_{\bar{q}}\tau_0 \gg 1$) a quasi unshifted phonon peak and a critical softening of the phonon frequency in the case of fast relaxation ($\omega_{\bar{q}}\tau_0 \ll 1$). In the intermediate case ($\omega_{\bar{q}}\tau_0 \simeq 1$) both the phonon frequency and the linewidth are strongly affected by the coupling. The behaviour of the [10] TA phonons in our molecular dynamics simulations is shown on Figures 2a and 2b where the transverse displacement–displacement response function $U(\bar{q}, \omega)$ are drawn for each accessible wavevector in the [01] direction and in Figures 3a and 3b where the actual phonon frequencies can be compared with the results of the orientational mean field calculation.

In the case of RUN A, the lowest TA mode (for $\bar{q} = [0.1, 0]$ in unit of $2\pi/a$) is lost in the wing of the central peak and there is a softening of the [10] TA frequencies with respect to the meanfield results which extends up to the zone boundary. In the case of RUN B, this softening of the [10] TA frequencies concerns only the long wavelength phonons (the two smallest accessible wavevectors).

In both cases, the phonon linewidth appears to be greatly enhanced whenever the phonon frequency matches with the librational frequencies. (The librational modes, which can be studied from the response functions of the collective variables associated with the orientational variables $\cos 2\theta$, show no wavevector dependence and the librational density of states has been drawn on Figures 1a and 1b in both cases of RUN A and RUN B. From I, we know that the linewidth of the librational density of states arrives mostly from static disorder effect.) This experimental correlation between phonon linewidth and librational density of states indicates the existence of a coupling between the [10] TA phonon and the librational modes. As the large amplitude librations participate strongly to the reorientational processes, this fact

†The small central resonance appearing in the longitudinal response function $U(\bar{q}, \omega)$ for $\bar{q}$ wavevector parallel to the [11] direction shows that the [11] LA branch is also slightly coupled to the rotations. Formula (III-8) shows that this coupling is maximum for the wavelengths which are halfway to zone boundary and Figure 5b shows that the corresponding phonon induces a breathing of the diagonal of the A^+ cage. However, the rotation-translation coupling is far less important in the case of the [11] LA branch than in the case of the [10] TA branch, partly because the geometrical coupling factor is weaker and partly because the bare phonon frequency of the [11] LA branch are higher than those of the [10] TA branch.

Downloaded by [Tomsk State University of Control Systems and Radio] at 13:23 20 February 2013

is in agreement with the general ideas of a reorientation-translation coupling theory.

Clearly, in the case of RUN A, the light moment of inertia of the dumbbell implies for the reorientational processes characteristic times τ_0 matching with the condition $\omega_{\vec{q}}\tau_0 \simeq 1$ over the whole [10] TA phonon branch. On the contrary, in the case of RUN B, the reorientational processes are slowed down by the high moment of inertia of the dumbbell so that the condition $\omega_{\vec{q}}\tau_0$ is fulfilled only for the long wavelength phonons. In that case, the [01] TA zone boundary phonons are still coupled to the rotational motion; however, they realize in fact a regime of slow relaxation ($\omega_{\vec{q}}\tau_0 \gg 1$).

V. ORIENTATIONAL CORRELATIONS

The correlations between neighbouring molecule orientations appear for instance in the spatial correlation $\Sigma_2(L)$ of the orientational pseudospin variable $\sigma_2(L)$ defined in (II-3)

$$\sigma_2(L) = 1 \times \text{sign of } \sin(2\theta_L)$$

$$\Sigma_2(L) = \Sigma_2(L, t = 0) = \left\langle \frac{1}{N}\sum_{L'}\sigma_2(L')\sigma_2(L' + L) \right\rangle \quad \text{(V-1)}$$

The pseudospin $\sigma_2(L)$ takes only two values ± 1 depending on which one of the two preferred orientations is actually the nearest from the instantaneous position of the molecule. The use of this function is in fact an efficient way of smearing out the librational oscillations in order to focus on the instantaneous equilibrium orientations and on the large reorientational motions of the molecules. The molecular dynamics results for the spatial correlation $\Sigma_2(L)$ appear in Table IIIa for RUN A and IIIb for RUN B, where the average square symmetry of the simulated sample has been a priori taken into account to improve on the statistics. These correlations appear to be very anisotropic and the presence of strong positive values along the [10] and [01] directions shows that the system tends to develop, along these directions, chains of ferro orientational ordered molecules. This result is, of course, not surprising in view of the instantaneous configurations of the simulated sample analysed in I: the structural fluctuations in the disorder system tend to locally reproduce the shear ferro-elastic distortion of the low temperature structure, and this distortion is obviously related to a ferro orientational ordering of the molecules along the [10] direction.

Downloaded by [Tomsk State University of Control Systems and Radio] at 13:23 20 February 2013

TABLE III

Spatial orientational correlation function $\Sigma_2(L_x, L_y)$.

IIIa for RUN A

L_y \ L_x	0	1	2	3	4	5
0	1	0.218	0.157	0.125	0.100	0.092
1		−0.033	−0.018	0.006	0.008	0.006
2			−0.060	−0.053	−0.053	−0.058
3				−0.061	−0.062	−0.078
4					−0.065	−0.075
5						−0.089

IIIb for RUN B

L_y \ L_x	0	1	2	3	4	5
0	1	0.156	0.114	0.088	0.067	0.069
1		−0.059	−0.023	0.002	−0.001	0.006
2			−0.050	−0.038	−0.037	−0.031
3				−0.039	−0.043	−0.036
4					−0.054	−0.043
5						−0.023

These spatial correlations reflect static properties of the system, they do not depend on the value of the moment of inertia and the results of the two runs can be compared: the correlations appear slightly more important in the case of RUN A which corresponds to a lower temperature (300 K) than in the case of RUN B (400 K). Assuming for the correlation function an exponential decay ($\lambda e^{-|L_x|/\xi}$), one obtains a good fit of the numerical data with the following value.

$$\lambda = 0.32 \qquad \xi = 2.6\, a \quad \text{for RUN A } (T = 300 \text{ K}) \qquad \text{(V-2a)}$$

$$\lambda = 0.23 \qquad \xi = 2.6\, a \quad \text{for RUN B } (T = 400 \text{ K}) \qquad \text{(V-2b)}$$

These results exhibit a normal increase of $\lambda(T)$ when the temperature approaches the ferroelastic transition and a surprising constant correlation length ξ, which is far from an usual mean field behaviour. Nevertheless, these numerical results must be considered with some caution in view of the small size of our sample Indeed, the above values of ξ imply that the exponential $\lambda e^{-|L_x|/\xi}$ is still far from zero when $|L_x|$ is half of the sample side length (i.e. when $|L_x| = 5a$), and, more precisely, the above results (V-2a) and (V-2b) arise from a fit of

Downloaded by [Tomsk State University of Control Systems and Radio] at 13:23 20 February 2013

the numerical data through the formula:

$$\Sigma_2(L) = \lambda[e^{-|L_x|/\xi} + e^{-|10-L_x|/\xi}] \qquad \text{(V-3)}$$

The effect of having a correlation length leading to static correlations which extend over more than half the size of the sample may lead to some spurious results which have not yet been analysed.

From a more fundamental point of view related to the structure of a plastic phase, the relative importance of those spatial orientational correlations in our simulation is partly an artefact arising from the low dimensionality of the system. In our two dimensional system, the molecules have only two possible preferred orientations (they have six ones in the real 3d cubic cyanide) and the steric hindrance in a two dimensional place is such an important constraint that even an indirect interaction (in our system the steric hindrance is only represented by the $A^+ - XY^-$ repulsive force) is sufficient to induce strong orientational correlations which are certainly less important in a real 3 dimensional case. In the framework of the linear coupling theory recalled in part III, these strong orientational correlations are described through a direct bilinear spin–spin interaction with an effective coupling coefficient $J(\bar{q})$ (*cf. formula III-1*). This effective spin–spin interaction can be thought as a renormalized term deriving from the non-linear part of the rotation-translation coupling. However, there is, for the moment, no theoretical predictions for the wavevector and temperature dependence of the coefficient $J(\bar{q})$. Thus it is not clear to decide whether the temperature independent correlation length $\xi(T)$ is simply the result of the small size of our sample or if it is also related to the temperature variations of the effective spin–spin interaction.

VI. COLLECTIVE REORIENTATIONAL MOTIONS

To investigate the collective behaviour of the reorientational processes we have computed the power spectra $S_2(\bar{q},\omega)$ and $\Sigma_2(\bar{q},\omega)$ of the collective, wave number dependent, variables $s_2(\bar{q})$ and $\sigma_2(\bar{q})$ associated respectively with the reorientational variables $\sin 2\theta_L$ and $\sigma_2(L)$:

$$S_2(\bar{q},\omega) = \int_{-\infty}^{+\infty} e^{-i\omega t}\langle s_2(\bar{q},t)s_2(\bar{q},0)^*\rangle \qquad \text{(VI-1)}$$

Downloaded by [Tomsk State University of Control Systems and Radio] at 13:23 20 February 2013

with $$s_2(\bar{q},t)=\frac{1}{\sqrt{N}}\sum_L e^{i\bar{q}\cdot\bar{R}_L}\sin 2\theta_L(t) \qquad \text{(VI-2)}$$

and $$\Sigma_2(\bar{q},\omega)=\int_{-\infty}^{+\infty} e^{-i\omega t}\langle\sigma_2(\bar{q},t)\sigma_2(\bar{q},0)^*\rangle \qquad \text{(VI-3)}$$

with $$\sigma_2(\bar{q},t)=\frac{1}{\sqrt{N}}\sum_L e^{i\bar{q}\bar{R}_L}\sigma_2(L,t) \qquad \text{(VI-4)}$$

For each value of $\bar{q}$ these spectra consist essentially of a central peak and, as expected, whatever is $\bar{q}$, the two functions $S_2(\bar{q},\omega)$ and $\Sigma_2(\bar{q},\omega)$ have the same lineshape within numerical errors. The main result of this section concerns their linewidth: the rotational spectra are actually found to be significantly narrower for the wavevector parallel to the [01] or [10] directions (which are precisely the privileged directions for the orientational correlations) than in any other direction. This is exemplified on Figure 6 where the power spectra $S_2(\bar{q},\omega)$ relative to the wave-vectors $\bar{q}=2\pi/a\ (0.1,0)$ and $\bar{q}=2\pi/a\ (0.1,0.1)$

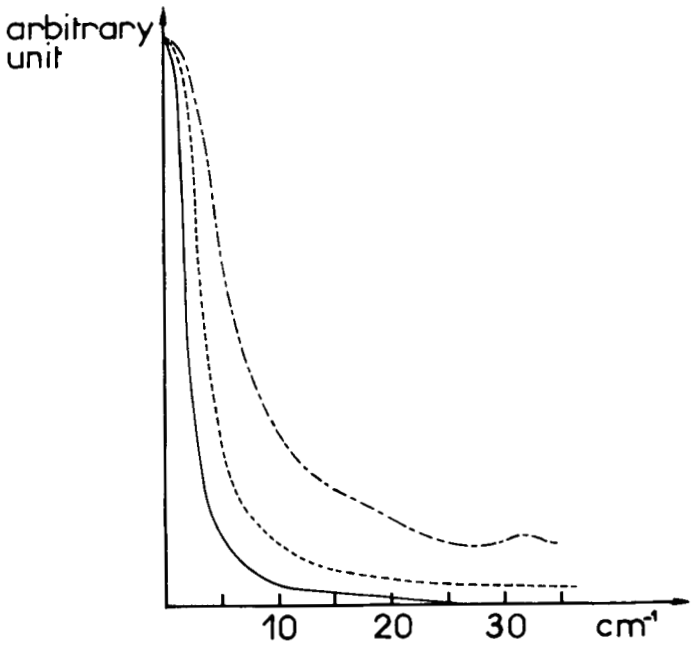

FIGURE 6 The Fourier spectra of orientational correlation functions (RUN B). Full line: $S_2(\bar{q},\omega)$ for $\bar{q}=2\pi/a$ [0.1, 0.0]; dashed line: The self orientation correlation function $S_2(\omega)=\int_{-\infty}^{+\infty}e^{i\omega t}\langle\sin 2\theta_L(t)\sin 2\theta_L(0)\rangle$. Dashed & dotted line: $S_2(\bar{q},\omega)$ for $\bar{q}=2\pi/a$ [0.1, 0.1].

Downloaded by [Tomsk State University of Control Systems and Radio] at 13:23 20 February 2013

are represented as well as the individual rotational correlation function $S_2(\omega)$.

This slowing down of the orientational fluctuations for wave-vectors parallel to [01] is obviously related to the rotation-translation coupling. This has been checked by looking for a central resonance in the displacement–displacement response functions $U(\bar{q}, \omega)$. As previously said in part IV, such a central component arises, very important, in the transverse response functions for $\bar{q}$ wavevectors parallel to the [10] direction and, far less important, in the longitudinal response functions when $\bar{q}$ is nearly half way to zone boundary along the [11] direction. The existence of such polarization effects in the translation-reorientation coupling was predicted by the analysis of our system via the K. H. Michel method (*cf.* III-8) and the Figures 5a and 5b help in understanding the physical origin of this selective rotation-translation coupling.

The translation-rotation coupling implies that the orientational correlation function and the central peak of the displacement–displacement response function should have the same lineshape for each value

TABLE IV

Correlation time $\tau(\bar{q})$ for $\bar{q}$ along the direction [10][a]

IVa is relative to RUN A					
q_x	0.1	0.2	0.3	0.4	0.5
$\tau_{\Sigma_2}(\bar{q})$	0.80	0.95	0.95	0.96	0.78
$\tau_{S_2}(\bar{q})$	0.81	0.90	1.02	0.95	0.86
$\tau_U(\bar{q})$	0.72	0.88	1.02	0.92	0.83
$\tau_{self} = 0.8$					
IVb is relative to RUN B					
q_x	0.1	0.2	0.3	0.4	0.5
$\tau_{\Sigma_2}(\bar{q})$	2.59	2.43	2.24	1.80	1.24
$\tau_{S_2}(\bar{q})$	2.62	2.50	2.31	1.84	1.26
$\tau_U(\bar{q})$	2.55	2.51	2.30	1.85	1.27
$\tau_{self} = 1.6$					

[a] $\tau_{\Sigma_2}(\bar{q})$, $\tau_{S_2}(\bar{q})$ and $\tau_U(\bar{q})$ are the correlation time deduced from the fit with the Lorentzian $I\tau/(1 + \omega^2\tau^2)$ of respectively: (a) the rotational power spectra $\Sigma_2(\bar{q}, \omega)$, (b) the rotational power spectra $S_2(\bar{q}, \omega)$, (c) the low frequency central component of the power spectra $U(\bar{q}, \omega)$ relative to the transverse displacement of the A^+ ions. τ_{self} is the correlation time of the self orientational correlation function $S_2(\omega)$, $\tau(\bar{q})$ is measured in 10^{-12} s, q_x is measured in unit of $2\pi/a$.

Downloaded by [Tomsk State University of Control Systems and Radio] at 13:23 20 February 2013

of the wavevector where the latter exists. This result has been checked, within the numerical accuracy of our calculation (*cf.* Table IV).

To get a more quantitative analysis of the reorientation-translation coupling we have fitted, for each wavevector $\bar{q}$ parallel to [10], the two rotational spectra $\Sigma_2(\bar{q}, \omega)$ and $S_2(\bar{q}, \omega)$ and the low frequency component of the transverse displacement–displacement spectra $U_t(\bar{q}, \omega)$ with a Lorentzian curve $I\tau/1 + \omega^2\tau^2$. Tables IV and V give respectively the correlation times $\tau_{\Sigma_2}(\bar{q})$, $\tau_{S_2}(\bar{q})$, $\tau_U(\bar{q})$ and the integrated intensity $I_{\Sigma_2}(\bar{q})$, $I_{S_2}(\bar{q})$ and $I_U(\bar{q})$ provided by this treatment.

As expected, for each wavevector $\bar{q}$, the three spectra $\Sigma_2(\bar{q}, \omega)$, $S_2(\bar{q}, \omega)$ and the low frequency component $U_t(\bar{q}, \omega)$ exhibit nearly the same correlation time which is simply called $\tau(\bar{q})$ in the following. The numerical value of $\tau(\bar{q})$ must be compared with the correlation time arising from the self rotational correlation function related to the

TABLE V

Integrated intensity for $\bar{q}$ along [10] of respectively, the rotational spectra $\Sigma_2(\bar{q}, \omega)$, the rotational spectra $S_2(\bar{q}, \omega)$, the central component of the power spectra $U(\bar{q}, \omega)$ relative to the transverse displacement of the A^+ ions[a]

Va is relative to RUN A					
q_x	0.1	0.2	0.3	0.4	0.5
$I_{\Sigma_2}(\bar{q})$	383	227	253	142	196
$\Sigma_2(\bar{q}, t = 0)$	326	235	261	173	201
$I_{S_2}(\bar{q})$	270	172	175	115	127
$S_2(\bar{q}, t = 0)$	225	164	177	126	129
$I_U(\bar{q})$	15.2	2.33	1.1	0.5	0.5
$U(\bar{q}, t = 0)$	12.4	2.46	1.3	0.7	0.6
Vb is relative to RUN B					
q_x	0.1	0.2	0.3	0.4	0.5
$I_{\Sigma^2}(\bar{q})$	239	202	190	193	110
$\Sigma_2(\bar{q}, t = 0)$	251	225	207	208	135
$I_{S_2}(q)$	165	142	134	133	77
$S_2(\bar{q}, t = 0)$	164	147	136	133	83
$I_U(\bar{q})$	8.3	1.9	1.1	0.7	0.5
$U(\bar{q}, t = 0)$	9.4	2.4	0.9	0.3	0.3

[a] $I_{\Sigma_2}(\bar{q})$, $I_{S_2}(\bar{q})$ and $I_U(\bar{q})$ are deduced from the fit of $\Sigma_2(\bar{q}, \omega)$, $S_2(\bar{q}, \omega)$ and the low frequency part of $U(\bar{q}, \omega)$ with the Lorentzian $I\tau/(1 + \omega^2\tau^2)$. They are measured in arbitrary unit but can be compared with the static correlation $\Sigma_2(\bar{q}, t = 0)$, $S_2(\bar{q}, t = 0)$ and $U(\bar{q}, t = 0)$. q_x is measured in unit of $2\pi/a$.

Downloaded by [Tomsk State University of Control Systems and Radio] at 13:23 20 February 2013

same angular variable $\sin 2\theta$. This time is approximately equal to 0.8 pcs in the case of RUN A and 1.6 pcs in the case of RUN B. The most striking fact is the behaviour of $\tau(\bar{q})$ as a function of the wavelength. In the case of RUN A, $\tau(\bar{q})$ is rather flat with a slight broad maximum when $\bar{q}$ is about half way to the zone boundary. On the contrary in the case of RUN B $\tau(\bar{q})$ decreases by a factor 2 from the zone center to the zone boundary. This behaviour is of course in relation with the change of the characteristic time for the rotational dynamics which has occurred between the two "experiments". This change appears clearly on the density of librational excitations which are shown on Figures 1a and 1b together with characteristic phonon dispersion curves. In the case of RUN A, the moment of inertia is small enough so that the librations (and thus the reorientations) are mixed up with the translational phonon nearly up to the zone boundary. In the second experiment (RUN B) the rotational dynamics is slowed down by a heavy moment of inertia of the molecules and only the phonons near to the zone center can be efficiently coupled to the orientational processes. In other words, the effective reorientation-translation coupling involves a balance between the geometrical aspect of the coupling potential which favors the zone boundary TA [10] phonon and the dynamical matching between the phonon frequencies and reorientational times which occurs only for the phonons near the zone center.

In Table V, the integrated intensity of the lorentzian extracted from our numerical fit $I_{\Sigma_2}(\bar{q})$, $I_{S_2}(\bar{q})$ and $I_U(\bar{q})$ is compared with the real integrated intensity of the power spectra $\Sigma_2(\bar{q},\omega)$, $S_2(\bar{q},\omega)$ and $U_t(\bar{q},\omega)$ (which are simply given by the $t = 0$ values of the corresponding correlation functions). The general agreement between these values shows the validity of our numerical fit. Besides these integrated intensities reflect, as already discussed in V, static quantities which are independent of the moment of inertia and the differences between the two runs only reflect the difference in temperature between the two cases.

It is finally important to compare our numerical results with the theoretical model of section III. In the slow relaxation regime this model predicts, on top of the proportionality between $U(\bar{q},\omega)$ and $\Sigma(\bar{q},\omega)$ (which is general for any linear model and has been checked above), the value of the proportionality constant

$$U_j(\bar{q},\omega) = \frac{|d_i(\bar{q})|^2}{\omega_j^4(\bar{q})}\Sigma(\bar{q},\omega) \qquad \text{(VI-1)}$$

Downloaded by [Tomsk State University of Control Systems and Radio] at 13:23 20 February 2013

and the variation of the relaxation time $\tau(\bar{q})$ with $\bar{q}$

$$\tau(\bar{q}) = \frac{\tau_0}{kT - J(\bar{q}) - \dfrac{|d_j(\bar{q})|^2}{\omega_j^2(\bar{q})}} \qquad \text{(VI-2)}$$

For the [10] TA branch, the value of $d_j(\bar{q})$ given in III-8 predicts that $d_j(\bar{q})$ is roughly proportional to q nearly up to the zone boundary, while $\omega_j(\bar{q})$ is also proportional to q. This means that the coefficient of proportionality in (VI-1) should behave as q^{-2}, while $\tau(\bar{q})$ should decrease with q as $|d_j(\bar{q})|^2/\omega_j^2(\bar{q})$ is roughly independent of q and $g(\bar{q}) = kT - J(\bar{q})$ is minimum for $q = 0$ (maximum of the spin–spin correlation function).

Both these predictions are approximately fulfilled for RUN B where $\tau(\bar{q})$ decreases with q, and $U_t(\bar{q}, \omega)/\Sigma(\bar{q}, \omega)$ behaves as q^{-2} for $q \geq 0.3\ a$ (*see* Tables IV and V). They are, on the contrary not fulfilled for RUN A, $\tau(\bar{q})$ being maximum for $q \simeq 0.3 \times 2\pi/a$. These results are clearly in line with our analysis of the dispersion curves for the T.A. branch. We already argued in section IV that the slow relaxation regime ($\omega_j(\bar{q})\tau_0 \gg 1$) was never achieved in the case of RUN A, while this regime was obtained for the T.A. branch for $q \gtrsim 0.3 \times 2\pi/a$ in the case of RUN B.

We thus obtain here an internal consistency of our results, which we shall briefly summarize in the conclusion.

VII. SUMMARY, DISCUSSION AND CONCLUSION

In this paper, second of a series devoted to a molecular dynamics study of a two dimensional model of an ODIC phase, we have addressed ourselves to the collective static and dynamical properties of our model. Three aspects of the problem have been studied here. The collective motions of the centers of mass (acoustical and optical phonon branches), the collective reorientational motions of the molecules, and finally the reorientation-translational coupling problem.

- The centers of mass motion has been found to be well described by a mean field theory, leading to well defined dispersion curves: the rather important phonon linewidth is essentially due to the static aspect of the disorder, characteristic of the plastic phases, the dynamical aspect of this disorder playing here an unimportant role.
- The model under study exhibits large orientational correlations along the [10] or [01] directions. The corresponding dynamical correla-

Downloaded by [Tomsk State University of Control Systems and Radio] at 13:23 20 February 2013

tions functions are well represented by Lorentzian, characteristic of collective reorientational processes describable in terms of a single, $\bar{q}$ dependent, relaxation time.

● The model exhibits a strong orientational-translation coupling which appears in various properties: a large anomalous Debye Waller factor, a softening of the [10] TA branch with an anomalous width of the corresponding phonons and the existence in the [10] transverse displacement–displacement response functions of a well defined central peak the behaviour of which is parallel to that of the reorientational correlation functions. This coupling is in turn responsible for the static correlations between the orientation of neighbouring molecules, as our model does not contain a direct coupling between these orientations.

We have also tried to analyse our data through the available theories pertinent to our problem. We have shown that the elementary approach of Glauber, Kubo, Huber and Yamada, which takes into account a bilinear coupling between a spin variable (which grossly describes the orientation of the dumbbell) and the center of mass motion can serve as a guide line to describe our results. Whenever the slow relaxation condition $\omega_j(\bar{q})\tau_0 \gg 1$ is met (where $\omega_j(\bar{q})$ is the frequency of a translation phonon which couples to the reorientation process, and τ_0 a mean life time of the spin in a given orientation), the results predicted by this theory are semi quantitatively obtained; results in qualitative agreement with this approach were also obtained for $\omega_j(\bar{q})\tau_0 \simeq 1$.

The theoretical basis of the preceding theory is nevertheless very weak for at least three different reasons:

a) it is a phenomenological theory, and thus it contains no procedure to compute the relevant quantities, in particular both the spin–spin and spin-phonon coupling parameters.

b) this theory artificially decouples the small amplitude motion of the centers of mass in the phonon regime and the large amplitude displacements of the same centers of mass related to the reorientation processes and the same is true for the orientational motion.

c) the translation-orientation coupling is linear in the displacement, a point which is partly (but only partly) related to the previous one.

The purpose of Michel, Naudts and de Raedt analysis can be seen as an effort to put this theory on a more quantitative basis, by providing a definite method for computing the relevant parameters of the theory, and a technique for deriving the correlation functions without a priori assuming a master equation for the orientational probability distribution function. We have in fact used their technique to evaluate the spin-phonon linear coupling parameter (*see* III and the

Downloaded by [Tomsk State University of Control Systems and Radio] at 13:23 20 February 2013

Downloaded by [Tomsk State University of Control Systems and Radio] at 13:23 20 February 2013

appendix) and so obtained qualitative agreement between the properties of our model and our molecular dynamic calculations. Unfortunately, by retaining only a term linear in the center of mass motion, this theory leads to a purely local spin–spin coupling, which does not fit at all with our results, and also predicts a temperature for the ferro elastic transition which is too high by a factor larger than 2 (*see* Appendix).

The inclusion of an orientation-translation coupling, quadratic in the translation variable is the most evident modification of the Michel *et al.* theory which could lead to a realistic evaluation of the effective orientation—orientation coupling coefficients. It is presently considered that such a modification provides a substantial improvement for the three dimensional case of NaCN (K. H. Michel *et al.*, *private communication*). The corresponding calculations, even in a two dimensional case, are already very lengthy and have not been performed yet.

In the absence of such results, it is not clear whether an expansion of the atomic displacement restricted to the first terms of this series is sufficient to describe both the phonon part and the reorientation-translation coupling, as it is implicitly assumed in the phenomenological theory. Simultaneously, it means that there is, for the time being no theoretical results to compare with our molecular dynamics data for the $\omega_j(\bar{q})\tau_0 \simeq$ regime.

Finally, the present paper has been completely devoted to the collective aspects of the residence time of the molecule in the "bottom of its potential well". The study of the two different runs has clearly demonstrated that the reorientational process is strongly related to the librational motion of the molecules. Nevertheless, the present study casts no light on the local processes which allows a molecule to overcome the steric hindrance due to the neighbouring atoms, or to stabilize finally in a new orientation. The study of the angular trajectory (*see* Figure 5a and Figure 5b of I) show that a given molecule can perform many $\pi/2$ rotations before falling into a new potential well, and this tendency seems more important, as the moment of inertia increases. A more sophisticated analysis of the reorientational process of the molecules and of the role of the local environment is thus clearly needed and will be the subject of a third paper of this series.

APPENDIX

We show here how the theory of K. H. Michel[5,6] for rotation-translation coupling can be applied to our two dimensional specific system.

In this theory, the orientational dependent part of the potential is expended in terms of the center of mass displacements, and the linear term of this development is, in turn, expended in terms of symmetry adapted function of the molecular orientations. This leads to a coupling potential which is bilinear in the center of mass displacement and in the orientational coordinate. Applying this scheme to our system, we give an estimation for the linear coupling coefficients. This treatment allows to evaluate first the softening of the acoustical [10] TA branch and second the transition temperature to an orientationally ordered phase. However the transition temperature provided by this method is in fact inconsistent with the behaviour of the system known from the numerical experiments.

a) The bilinear rotation-translation coupling term

In our system, the orientational dependent part of the potential arises uniquely from the short range repulsive interaction and writes

$$V = \sum_{L} \sum_{L'}{}' \sum_{s=\pm 1} \lambda e^{-|\bar{R}_-(L) + s\bar{d}(L) - \bar{R}_+(L')|/r_0} \tag{A-1}$$

with the following conventions

the two (A^+ and XY^-) ions in each unit cell L are labelled $L_\pm$.

the vector $\bar{R}_\pm(L)$ gives the position of the centers of mass which can be expressed in terms of the equilibrium position $\bar{X}_\pm(L)$ plus the displacement $\bar{u}_\pm(L)$

$$\bar{R}_\pm(L) = \bar{X}_\pm(L) + \bar{u}_\pm(L) \tag{A-2}$$

the vector $\bar{d}(L)$ of coordinates $(d/2\cos\theta_L, d/2\sin\theta_L)$ gives the position of the ends of the dumbbell (L_-).

The sum over L runs over all the unit cell of the sample, while the sum over L' is restricted to the cell including the nearest neighbour of the (L_-) ions.

Following K. H. Michel, this potential is expended in terms of the displacements $\bar{u}_\pm(L)$. The zero order term depends only on the molecular orientations:

$$V_R = \sum_L V_R(L)$$

with

$$V_R(L) = \sum_{L'}{}' 2\lambda e^{-|\bar{X}_-(L) + \bar{d}(L) - \bar{X}_+(L')|/r_0} \tag{A-3}$$

Downloaded by [Tomsk State University of Control Systems and Radio] at 13:23 20 February 2013

On our two dimensional system, the symmetry adapted functions for the molecular orientations are simply the trigonometric function $\cos n\theta$ and $\sin n\theta$. Owing to the square symmetry of the lattice of equilibrium center of mass position, the development of this term writes simply

$$V_R(L) = \lambda\left(\alpha_0^0 + \sum_{p=1}^{\infty} \alpha_{4p}^0 \cos 4p\theta_L\right) \tag{A-4}$$

The first order term in displacement writes:

$$V_{TR} = -\sum_L \sum_{L'}{}' \bar{P}_{(1)}(LL', \theta_L) \cdot (\bar{u}_-(L) - \bar{u}_+(L')) \tag{A-5}$$

with

$$\bar{P}_{(1)}(LL', \theta_L) = \frac{\lambda}{r_0} \sum_{s=\pm 1} e^{-|\bar{X}^s_{LL'}|/r_0} \frac{\bar{X}^s_{LL'}}{|\bar{X}^s_{LL'}|} \tag{A-6}$$

$$\bar{X}^s_{LL'} = \bar{X}_-(L) + s\bar{d}(L) - \bar{X}_+(L') \tag{A-7}$$

Owing to the square symmetry V_{TR} simplifies to

$$V_{TR} = \sum_L \sum_{L'}{}' \bar{P}_{(1)}(LL', \theta_L) \bar{u}_+(L') \tag{A-8}$$

Now the term $\bar{P}_{(1)}(LL', \theta_L)$ is expended in trigonometric Fourier series: owing to the head-tail symmetry of the dumbbells this expansion includes only even order terms ($\cos 2p\theta_L, \sin 2p\theta_L$) and owing to the square symmetry of the equilibrium lattice the $p = 0$ term does not contribute to the sum in (A-8). Thus, the rotation-translation coupling term writes:

$$V_{TR} = \sum_{p \neq 0} \sum_L \sum_{L'}{}' u_+^\alpha(L) v_{2p}^{\alpha m}(LL') C_{2p}^m(\theta_L) \tag{A-9}$$

where α labels the cartesian components

$m = 1, 2$ labels the two $2p$ trigonometric function:

$$C_{2p}^1(\theta) = \cos 2p\theta \text{ and } C_{2p}^2(\theta) = \sin 2p\theta$$

and

$$v_{2p}^{\alpha m}(LL') = \frac{1}{\pi} \int_0^{2\pi} P_{(1)}^\alpha(L, L', \theta_L) C_{2p}^m(\theta_L)\, d\theta_L \tag{A-10}$$

Downloaded by [Tomsk State University of Control Systems and Radio] at 13:23 20 February 2013

Equation (A-9) thus provides a rotation-translation coupling potential which is bilinear in terms of the center mass displacement and of the orientational variables $C_{2p}^{m}(\theta)$.

The next point is to perform, first, a spatial Fourier transform:

$$\bar{u}_{\pm}(\bar{q}) = \frac{1}{\sqrt{N}} \sum_{L} e^{i\bar{q}\cdot\bar{X}_{\pm}(L)} \bar{u}_{\pm}(L) \tag{A-11}$$

$$C_{2p}^{m}(\bar{q}) = \frac{1}{\sqrt{N}} \sum_{L} e^{i\bar{q}\cdot\bar{X}_{-}(L)} C_{2p}^{m}(\theta_L) \tag{A-12}$$

$$v_{2p}^{\alpha m}(\bar{q}) = \sum_{L'}{}' v_{2p}^{\alpha m}(LL')\, e^{i\bar{q}\cdot(\bar{X}_{+}(L') - \bar{X}_{-}(L))} \tag{A-13}$$

leading to

$$V_{TR} = \sum_{\bar{q}} u_{+}^{\alpha}(-\bar{q})\, v_{2p}^{\alpha m}(\bar{q})\, C_{2p}^{m}(\bar{q}) \tag{A-14}$$

and second the projection which, at least for $\bar{q} = 0$ separates the center of mass displacement from the optic mode:

$$\begin{pmatrix} \bar{s}_a(\bar{q}) \\ \bar{s}_0(\bar{q}) \end{pmatrix} = \begin{bmatrix} \sqrt{\frac{m_+}{m}} & \sqrt{\frac{m_-}{m}} \\ \sqrt{\frac{m_-}{m}} & -\sqrt{\frac{m_+}{m}} \end{bmatrix} \begin{pmatrix} \sqrt{m}_{+}\, \bar{u}_{+}(\bar{q}) \\ \sqrt{m}_{-}\, \bar{u}_{-}(\bar{q}) \end{pmatrix} \tag{A-15}$$

$$\begin{pmatrix} v_{a2p}^{\alpha m}(\bar{q}) \\ v_{02p}^{\alpha m}(\bar{q}) \end{pmatrix} = \begin{bmatrix} \sqrt{\frac{m_+}{m}} & \sqrt{\frac{m_-}{m}} \\ \sqrt{\frac{m_-}{m}} & -\sqrt{\frac{m_+}{m}} \end{bmatrix} \begin{pmatrix} \frac{1}{\sqrt{m_+}} v_{2p}^{\alpha m}(\bar{q}) \\ 0 \end{pmatrix} \tag{A-16}$$

with $m = m_{+} + m_{-}$. We finally get the translation-rotation coupling term under the form

$$V_{TR} = \sum_{\bar{q}} s_{\rho}^{\alpha}(-\bar{q})\, v_{\rho 2p}^{\alpha m}(\bar{q})\, C_{2p}^{m}(\bar{q}) \tag{A-17}$$

where the index $\rho = a, o$ labels the optic and acoustic projection of the displacement.

In our system, the four A^{+} ions neighbouring one XY^{-} dumbbell are located at the vectors $\bar{X}_{\pm}(L') - \bar{X}_{-}(L) = (\epsilon_x a/2, \epsilon_y a/2)$ with

Downloaded by [Tomsk State University of Control Systems and Radio] at 13:23 20 February 2013

$\epsilon_x = \pm 1$, $\epsilon_y = \pm 1$ we have

$$v_{2p}^{\alpha m}(\epsilon_x a/2, \epsilon_y a/2) = \begin{matrix} \\ \alpha = x \\ \alpha = y \end{matrix} \begin{pmatrix} m = 1 & m = 2 \\ \epsilon_x A_{2p} & -\epsilon_y (-1)^p B_{2p} \\ \epsilon_y (-1)^p A_{2p} & \epsilon_x B_{2P} \end{pmatrix} \tag{A-18}$$

A_{2p} and B_{2p} can be computed from (A-6), (A-7) and (A-10).

Of course, only the $p = 1$ term will have important numerical values (indeed, important term for higher p values would imply for the rotation-translation potential fast variation with respect to the angular coordinate which are not realistic) and with the numerical value of our simulation (*listed in* table I) we obtain

$$A_2 = 4.41\ 10^{-11}\ \text{MKSA} \tag{A-19}$$

$$B_2 = 1.86\ 10^{-10}\ \text{MKSA} \tag{A-20}$$

The spatial Fourier transform leads to

$$\sqrt{m} v_{a2p}^{\alpha m}(\bar{q}) = v_{2p}^{\alpha m}(\bar{q})$$

$$\begin{matrix} \\ \alpha = x \\ \alpha = y \end{matrix} \left[\begin{pmatrix} m = 1(\cos 2p\theta) & m = 2(\sin 2p\theta) \\ A_{2p} \sin q_x \frac{a}{2} \cos q_y \frac{a}{2} & -(-1)^p B_{2p} \cos q_x \frac{a}{2} \sin q_y \frac{a}{2} \\ (-1)^p A_{2p} \cos q_x \frac{a}{2} \sin q_y \frac{a}{2} & B_{2p} \sin q_x \frac{a}{2} \cos q_y \frac{a}{2} \end{pmatrix} \right] \quad 4i \tag{A-21}$$

From the expression (A-21) of the bilinear rotation-translation coupling term it is clear that:

1) in the [10] wave vector direction ($q_y = 0$) the reorientational variable $\sin 2\theta$ couples to the transverse (y) displacement mode only and the coupling coefficient is maximum for the zone boundary phonon $q_x = \pi/a$.

2) in the [11] wave vector direction ($q_x = q_y$) the reorientational variable $\sin 2\theta$ couples to the longitudinal mode and the coupling is maximum halfway to the zone boundary.

These results are indeed consistent with the behaviour of our simulated system (*cf.* part IV).

Downloaded by [Tomsk State University of Control Systems and Radio] at 13:23 20 February 2013

Downloaded by [Tomsk State University of Control Systems and Radio] at 13:23 20 February 2013

b) Softening of the shear elastic constant C_{44} and the transition temperature

Still following the work of K. H. Michel we study now the static susceptibilities of the system in the linear response approximation. For this purpose, we assume that the potential energy of the system can be written as a sum of three terms:

■ an usual harmonic phonon contribution

$$V_t = \frac{1}{2} \sum_{\bar{q}, \rho = a, o} \bar{S}_\rho(-\bar{q}) \bar{\bar{M}}_\rho(\bar{q}) \bar{S}_\rho(\bar{q}) \tag{A-22}$$

we assume here that the acoustic and optic mode decouple which is at least true for small $\bar{q}$ values which we are going to be interested in here.

■ the rotation-translation bilinear coupling term derived above

$$V_{TR} = \sum_{\bar{q}} s_\rho^\alpha(-\bar{q}) v_{\rho 2p}^{\alpha m}(\bar{q}) C_{2p}^m(\bar{q}) \tag{A-23}$$

■ the pure rotational term V_R written in (A-3) and (A-4). If the pure rotational term V_R should be considered alone, it would lead to a static orientation susceptibility which does not depend on the wave vector and can be written:

$$\left(C_{2p}^m(-\bar{q}), C_{sp'}^{m'}(\bar{q})\right) = \beta R_{2p2p'}^{mm'} \tag{A-24}$$

with

$$R_{2p2p'}^{mm'} = \frac{\int e^{-V_R(\theta_L)} C_{2p}^m(\theta_L) C_{2p'}^{m'}(\theta_L)\, d\theta_L}{\int e^{-V_R(\theta_L)}\, d\theta_L} \tag{A-25}$$

$$\beta = \frac{1}{kT}$$

In the limit of the linear response approximation, the potential V_R can be replaced by the harmonic term which gives rise to the same static correlation i.e.

$$V_R = \frac{1}{2\beta} \sum_{\bar{q}} C_{2p}^m(-\bar{q}) (R^{-1})_{2p2p'}^{mm'} C_{2p'}^{m'}(\bar{q}) \tag{A-26}$$

In the following we are merely interested in the anomalous elastic behaviour of the crystal which arises from the rotation-translation coupling. We are therefore interested in the long wavelength behaviour of correlation functions. We shall neglect the coupling of the rotations to the optic modes and the optic modes will be dropped in (A-22) and (A-23). Besides we shall in (A-22) to (A-26) retain only the rotational variables $\sin 2\theta$ and $\cos 2\theta$ which correspond to the $p = 1$ terms.

Under these conditions, the potential energy of the coupled system reads:

$$H_p = \frac{1}{2}\sum_{\bar{q}}\Big(\bar{s}(-\bar{q})\bar{\bar{M}}(\bar{q})\bar{s}(\bar{q}) + \bar{s}(-\bar{q})\tilde{\bar{v}}(\bar{q})\tilde{C}_2(\bar{q}) + \frac{1}{\beta}\tilde{C}_2(-\bar{q})\tilde{\bar{R}}_2^{-1}C_2(\bar{q})\Big) \tag{A-27}$$

where we have used an obvious matrix notation and dropped the subscript a for acoustic modes.

Now the static susceptibilities of the coupled system are just obtained through the inverse of the matrix

$$\begin{array}{c} \\ \bar{s} \\ \tilde{C}_2 \end{array}\begin{array}{c} \begin{array}{cc} \bar{s} & \tilde{C}_2 \end{array} \\ \begin{pmatrix} \bar{\bar{M}}(\bar{q}) & \tilde{\bar{v}}(\bar{q}) \\ \tilde{\bar{v}}^t(-\bar{q}) & \dfrac{1}{\beta}\tilde{\bar{R}}_2^{-1} \end{pmatrix} \end{array} \tag{A-28}$$

Therefore, we obtain for the static displacement–displacement susceptibility

$$\bar{\bar{D}}^{-1}(\bar{q}) = (\bar{s}(-\bar{q})\bar{s}(\bar{q})) = \left[\bar{\bar{M}}(\bar{q}) - \beta\tilde{\bar{v}}(\bar{q})\tilde{\bar{R}}_2\tilde{\bar{v}}^t(-\bar{q})\right]^{-1} \tag{A-29}$$

and for the rotational static susceptibility $\Gamma(\bar{q})$

$$kT\Gamma^{-1}(\bar{q}) = kT\tilde{\bar{R}}_2^{-1} - \tilde{\bar{v}}^t(-\bar{q})\bar{\bar{M}}^{-1}(\bar{q})\tilde{\bar{v}}(\bar{q}) \tag{A-30}$$

As it is well known, in the long wavelength limit the static displacement–displacement susceptibility is related to the elastic constant: in a two dimensional system this relation reads

$$D_{ij}(\bar{q}) = \frac{s_2}{m}C_{ijkl}q_kq_l \tag{A-31}$$

Downloaded by [Tomsk State University of Control Systems and Radio] at 13:23 20 February 2013

where s_2 is the surface of the unit cell, and $m = m_+ + m_-$ the total mass.

The matrix $M(\bar{q})$ is related to what would be the elastic constant C_{ijkl} if there was no coupling between the phonons and the reorientation (the bare elastic constant). Equation (A-29) describes thus the anomalous elastic behaviour of the crystal while (A-30) expresses the renormalization of the orientational potential owing to translation-rotation coupling. It should perhaps be noted here that equation (5-16) and (6-1) of Ref. 5 can be casted in a form similar to (A-29) and (A-30).

For a $\bar{q}$ wave vector parallel to [10] ($q_y = 0$) and in the long wavelength limit (q_x small), we get: from (A-31)

$$\bar{\bar{D}}(\bar{q}) = \frac{s_2}{m}\begin{pmatrix} c_{11}q_{x^2} & 0 \\ 0 & c_{44}q_{x^2} \end{pmatrix} \tag{A-32}$$

$$\bar{\bar{M}}(\bar{q}) = \frac{s_2}{m}\begin{pmatrix} c^0_{11}q_{x^2} & 0 \\ 0 & c^0_{44}q_{x^2} \end{pmatrix} \tag{A-33}$$

from (A-21)

$$\tilde{\bar{v}}(\bar{q}) = \frac{2i}{\sqrt{m}}\begin{pmatrix} A_2q_x & 0 \\ 0 & B_2q_y \end{pmatrix} \tag{A-34}$$

and from (A-25)

$$\beta\tilde{\bar{R}}_2 = \frac{\beta}{4}\begin{pmatrix} 2 + a^0_4 & 0 \\ 0 \quad 2 & -a^0_4 \end{pmatrix} \tag{A-35}$$

where a^0_4 is the first relevant coefficient trigonometric Fourier series of the probability $P_0(\theta)\alpha e^{-\beta V}R^{(\theta)}$ associated with the potential $V_R(\theta)$

$$P_0(\theta)\alpha e^{-\beta V}R^{(\theta)} = \frac{1}{2\pi} + \alpha^0_4(T)\cos 4\theta + \cdots \tag{A-36}$$

Then, equations (A-39) and (A-30) can be rewritten as

$$c_{11} = c^0_{11} - \frac{A_2^2}{kT}(2 + a^0_4(T)) \tag{A-37}$$

$$c_{44} = c^0_{44} - \frac{B_2^2}{kT}(2 - a^0_4(T)) \tag{A-38}$$

Downloaded by [Tomsk State University of Control Systems and Radio] at 13:23 20 February 2013

and

$$(kT)\tilde{\tilde{\Gamma}}^{-1} = 4\begin{pmatrix} \dfrac{kT}{(2 + a_4^0(T))} - \dfrac{A_2^2}{c_{11}^0} & 0 \\ 0 & \dfrac{kT}{(2 - a_4^0(T))} - \dfrac{B_2^2}{c_{44}^0} \end{pmatrix} \tag{A-39}$$

Now, there is no precise definition of what are the "bare" elastic constant c_{11}^0 and c_{44}^0. However, as an estimate, we can take the values which correspond to the mean field dispersion curves which have been calculated in section IV. This leads to:

$$c_{44}^0 = 6.67 \quad \text{MKSA} \tag{A-40}$$

$$c_{11}^0 = 20.7 \quad \text{MKSA} \tag{A-41}$$

which, in view of the value of A_2 and B_2 (*given in* (A-19) and (A-20)) leads to

$$\frac{B_2^2}{kc_{44}^0} = 378\ K \quad \text{and} \quad \frac{A_2^2}{kc_{11}^0} = 684\ \text{K} \tag{A-42}$$

The potential $V_R(\theta)$ corresponding to the numerical values used in our calculation has been computed together with the first coefficients of the development (A-4). It can be, in fact, fairly well be represented by its two first terms:

$$V_R(L) = \lambda\alpha_0^0 + \lambda\alpha_4^0 \cos 4\theta \tag{A-43}$$

with

$$\frac{\lambda\alpha_4^0}{k} = 74\ \text{K} \tag{A-44}$$

Then, equation (A-36) leads to

$$a_4^0(T) = -\frac{2I_1\left(\dfrac{\lambda\alpha_4^0}{kT}\right)}{I_0\left(\dfrac{\lambda\alpha_4^0}{kT}\right)} \tag{A-45}$$

Downloaded by [Tomsk State University of Control Systems and Radio] at 13:23 20 February 2013

where I_0 and I_1 are modified Bessel functions of the first kind. The value (A-45) for $a_4^0(T)$, together with equations (A-38) and (A-39) imply that c_{44} will reach zero and the orientational susceptibility Γ will diverge for a temperature T_c which is about 700 K. This result is of course inconsistent with our numerical experiments where it appears that the system was still in a disordered phase at the temperatures of 300 K (RUN A) and 400 K (RUN B). Besides, equation (A-38) leads to static orientational susceptibilities Γ which are independent of the wave vector, results which clearly do not fit at all with our numerical data for the static orientational correlations (*cf.* tables IV and V).

References

1. S. Haussuhl, J. Eckstein, K. Recker and F. Wallrafen, *Acta Cryst.* **A33**, 847 (1977).
2. M. Boissier, R. Vacher, D. Fontaine and R. M. Pick, *J. Physique* **41**, 1437 (1980).
3. J. J. Rush, J. M. Rowe, N. Vagelatos, D. L. Price, D. G. Hinks and S. Susman, *J. Chem. Phys.* **62**, 4551 (1975).
4. R. J. Glauber, *J. Math. Phys.* **4**, 294 (1963). Y. Yamada, H. Takatera and D. L. Huber, *J. Phys. Soc. Japan* **36**, 641 (1974).
5. K. H. Michel and J. Naudts, *J. Chem. Phys.* **67**, 547 (1977).
6. K. H. Michel and J. Naudts, *J. Chem. Phys.* **68**, 216 (1978).
7. B. de Raedt and K. H. Michel, *Discuss. Faraday Soc.* **69**, 88 (1980).
8. M. L. Klein and J. J. Weis, *J. Chem. Phys.* **67**, 217 (1977).
9. M. L. Klein, D. Levesque and J. J. Weis, *J. Chem. Phys.* **74**, 2566 (1981).
10. G. S. Pawley and G. W. Thomas, *Phys. Rev. Letters* **48**, 410 (1982).
11. D. G. Bounds, M. L. Klein and I. R. McDonald, *Phys. Rev. B* **24**, 3568.
12. M. L. Klein, Y. Ozaki and I. R. McDonald, *J. Phys. C* **15**, 4993 (1982).
13. M. L. Klein and I. R. McDonald, *Chem. Phys. Letters* **78**, 383 (1981).
14. R. M. Lynden-Bell, I. R. McDonald and M. L. Klein, *Mol. Phys.* **48**, 1093 (1983).
15. M. Yvinec, *Mol. Cryst. Liq. Cryst.* **89**, 359 (1982).
16. S. G. Brush, H. L. Sahlin and E. Teller, *J. Chem. Phys.* **45**, 2102 (1966).
17. L. Verlet, *Phys. Rev.* **159**, 98 (1967).

Downloaded by [Tomsk State University of Control Systems and Radio] at 13:23 20 February 2013